Eddies reduce denitrification and compress habitats in the Arabian Sea

Zouhair Lachkar, K. Shafer Smith, Marina Lévy, Olivier Pauluis

AGU PUBLICATIONS

Geophysical Research Letters

RESEARCH LETTER
10.1002/2016GL069876

Key Points:
- Lateral eddy transport of dissolved oxygen plays a lead role in ventilating the Arabian Sea Oxygen Minimum Zone (OMZ)
- By reducing the extent of the suboxic zone, eddies limit denitrification and hence increase ecosystem primary production
- Enhanced productivity amplifies O_2 consumption in the subsurface, leading to an expansion of hypoxia and a compression of habitats

Supporting Information:
- Supporting Information S1

Correspondence to:
Z. Lachkar,
zouhair.lachkar@nyu.edu

Citation:
Lachkar, Z., S. Smith, M. Lévy, and O. Pauluis (2016), Eddies reduce denitrification and compress habitats in the Arabian Sea, *Geophys. Res. Lett.*, *43*, 9148–9156, doi:10.1002/2016GL069876.

Received 6 JUN 2016
Accepted 12 AUG 2016
Accepted article online 16 AUG 2016
Published online 4 SEP 2016

Eddies reduce denitrification and compress habitats in the Arabian Sea

Zouhair Lachkar[1], Shafer Smith[1,2], Marina Lévy[3], and Olivier Pauluis[1,2]

[1]Center for Prototype Climate Modeling, New York University Abu Dhabi, Abu Dhabi, UAE, [2]Courant Institute of Mathematical Sciences, New York University, New York, USA, [3]Sorbonne Université (UPMC Paris 6/CNRS/IRD/MNHN), LOCEAN-IPSL, Paris, France

Abstract The combination of high biological production and weak oceanic ventilation in regions, such as the northern Indian Ocean and the eastern Pacific and Atlantic, cause large-scale oxygen minimum zones (OMZs) that profoundly affect marine habitats and alter key biogeochemical cycles. Here we investigate the effects of eddies on the Arabian Sea OMZ—the world's thickest—using a suite of regional model simulations with increasing horizontal resolution. We find that isopycnal eddy transport of oxygen to the OMZ region limits the extent of suboxia so reducing denitrification, increasing the supply of nitrate to the surface, and thereby enhancing biological production. That same enhanced production generates more organic matter in the water column, amplifying oxygen consumption below the euphotic zone, thus increasing the extent of hypoxia. Eddy-driven ventilation likely plays a similar role in other low-oxygen regions and thus may be crucial in shaping marine habitats and modulating the large-scale marine nitrogen cycle.

1. Introduction

Oceanic concentrations of oxygen are set by a competition between physical transport and biological consumption: oxygen dissolved into the ocean's surface is transported downward by ocean currents (ventilation) and consumed as an oxidant in the bacterial decomposition of organic matter (remineralization) that is the byproduct of planktonic production. In regions where productivity is high and ventilation is weak, as is the case in the northern Indian Ocean and the eastern tropical Pacific and Atlantic, the limited replenishment of oxygen depleted by remineralization results in large oxygen minimum zones (OMZs). These have profound effects on marine habitats and biogeochemical cycles [*Codispoti et al.*, 2001; *Gray et al.*, 2002; *Vaquer-Sunyer and Duarte*, 2008; *Gruber*, 2011]: at moderate levels of oxygen deficiency (hypoxia) the growth, survival, and reproductive success of higher trophic animals such as crustacea and fishes are impeded; at even lower oxygen levels (suboxia), nitrate replaces oxygen (denitrification) as the oxidant in remineralization, depleting the inventory of bioavailable nitrogen, the main macronutrient of marine productivity. Mesoscale and submesoscale eddies complicate the picture further, affecting both biological production and ventilation rates in several oxygen-depleted zones [*Falkowski et al.*, 1991; *Oschlies and Garçon*, 1998; *Lévy et al.*, 2001; *Gruber et al.*, 2011; *Resplandy et al.*, 2011; *McCreary et al.*, 2013; *Duteil et al.*, 2014; *Bettencourt et al.*, 2015] in ways that remain poorly understood.

Several studies have demonstrated that mesoscale and submesoscale phenomena enhance biological productivity in oligotrophic open ocean environments [*Falkowski et al.*, 1991; *McGillicuddy et al.*, 1998; *Oschlies and Garçon*, 1998; *Lévy et al.*, 2001] and suppress it in eastern boundary coastal upwelling systems [*Lathuilière et al.*, 2010, 2011; *Gruber et al.*, 2011; *Lachkar and Gruber*, 2011]. On the other hand, other studies have suggested that eddies enhance ocean mixing in regions of sluggish circulation in the Atlantic and Pacific shadow zones and in the North Indian Ocean, potentially contributing to the ventilation of oxygen deficient zones [*Resplandy et al.*, 2011; *McCreary et al.*, 2013; *Gnanadesikan et al.*, 2013; *Brandt et al.*, 2015; *Bettencourt et al.*, 2015]. This complex role of eddies poses an especially difficult challenge for eddy parameterizations used in coarse resolution simulations—the large discrepancies between observations of OMZs and their representation in global ocean models suggest that this challenge has not yet been met [*Gnanadesikan et al.*, 2013; *Cabré et al.*, 2015]. An extensive understanding of the role of eddies in low-oxygen environments is therefore needed to improve its parameterization and thus predictions of global oxygen distributions in future oceans and climate.

In the Arabian Sea, eddies have been suggested to play an important role in the oxygen [*Resplandy et al.*, 2011; *McCreary et al.*, 2013] and nutrient [*Resplandy et al.*, 2012] budgets. Yet the integrated effects of eddies on the intensity and size of the Arabian Sea OMZ have remained largely unknown, and their biogeochemical and ecological implications are still poorly understood. In order to explore the effects of eddies on oxygen distribution in the Arabian Sea, we performed a series of regional simulations using the Regional Oceanic Modeling System (ROMS) model [*Shchepetkin and McWilliams*, 2005] coupled to a nutrient-phytoplankton-zooplankton-detritus (NPZD) ecosystem model that includes a module describing oxygen transformations and a parameterization of denitrification [*Gruber et al.*, 2006]. The seasonal mean distributions of the model-simulated key physical and biogeochemical properties show a decent agreement with several observational constraints, indicating a sufficient degree of realism for the purpose of this study (see supporting information). We performed simulations of the Arabian Sea at four horizontal resolutions: 1/3°, 1/6°, 1/12°, and 1/24°. As the level of eddy activity simulated in each experiment is proportional to the model resolution, contrasting the low- and high-resolution simulations allows us to quantify the net effects of eddies on circulation and the biogeochemical cycling in the Arabian Sea. Details of the model and the tests discussed here are provided in section 2 and in the supporting information.

2. Methods

2.1. The Models

We use the version 3.1.1 of the Regional Oceanic Modelling System (ROMS) — Agrif (documented in detail at http://www.romsagrif.org/). ROMS is a free-surface, primitive equation model that is formulated in horizontal curvilinear coordinates and uses a terrain-following vertical coordinate [*Shchepetkin and McWilliams*, 2005]. Advection is formulated using a rotated-split third-order upstream biased operator following *Marchesiello et al.* [2009]. This scheme has been shown to limit dispersion and preserve low diffusion. The subgrid vertical mixing is parameterized using the nonlocal K-Profile Parameterization (KPP) scheme [*Large et al.*, 1994]. No background lateral diffusivity is used, and the dissipation of small-scale noise is ensured by numerical diffusivity only. Because our primary goal is to identify the role of resolved eddies through comparisons of eddying and noneddying runs, no Gent-McWilliams [*Gent and McWilliams*, 1990] eddy parameterization is used. The biogeochemical model is a nutrient-phytoplankton-zooplankton-detritus (NPZD) model based on nitrogen [*Gruber et al.*, 2006]. The ecological model is augmented with an oxygen cycle module that is described in the supporting information. The sinking particulate organic matter that reaches the seafloor is retained in a sediment layer, where it is subjected to a slower remineralization rate than in the water column. Both water column and benthic denitrification at low-oxygen concentration are represented in the model (see further details in the supporting information).

2.2. The Experimental Setup

The model domain covers the area extending from 5°S to 30°N in latitude and from 32°E to 78°W in longitude. The vertical grid contains 32 levels with refined resolution near the surface. The model was run at four different horizontal resolutions: 1/3°, 1/6°, 1/12°, and 1/24°. The bathymetry is based on the ETOPO2 file from the National Geophysical Data Center [*Smith and Sandwell*, 1997]. The topography is smoothed to avoid large-pressure gradient errors. Sea floor minimum depth is set to 20 m. The model is forced with climatological monthly forcing. The initial and lateral boundary conditions for oxygen and nitrate are based on the World Ocean Atlas 2009. The lateral boundary conditions for currents, temperature, and salinity are derived from the Simple Ocean Data Assimilation ocean reanalysis. The surface heat and freshwater fluxes are taken from the Comprehensive Ocean-Atmosphere Data Set (COADS) [*da Silva et al.*, 1994]. Surface temperature and salinity are restored to COADS observations using a kinematic heat and freshwater flux corrections following *Barnier et al.* [1995]. Wind stress is calculated from the QuikSCAT-derived Scatterometer Climatology of Ocean Winds [*Risien and Chelton*, 2008]. The model is spun up for 20 years. For model evaluation and oxygen budgets, we generally use the model years 13 to 20 during which the model drift in O_2 becomes small and the differences between the low- and high-resolution simulations are stable over time (see Figure S1 in the supporting information).

2.3. Summary of Model Evaluation

The model performance is quantified for both the lowest (1/3°) and the highest (1/24°) resolutions using a wide array of satellite and in situ observations (see Figures S2 and S3 in the supporting information). The highest-resolution simulation (1/24°) shows consistently a higher skill with better correlations with observations and a better representation of the observed variance for both physical and biogeochemical variables.

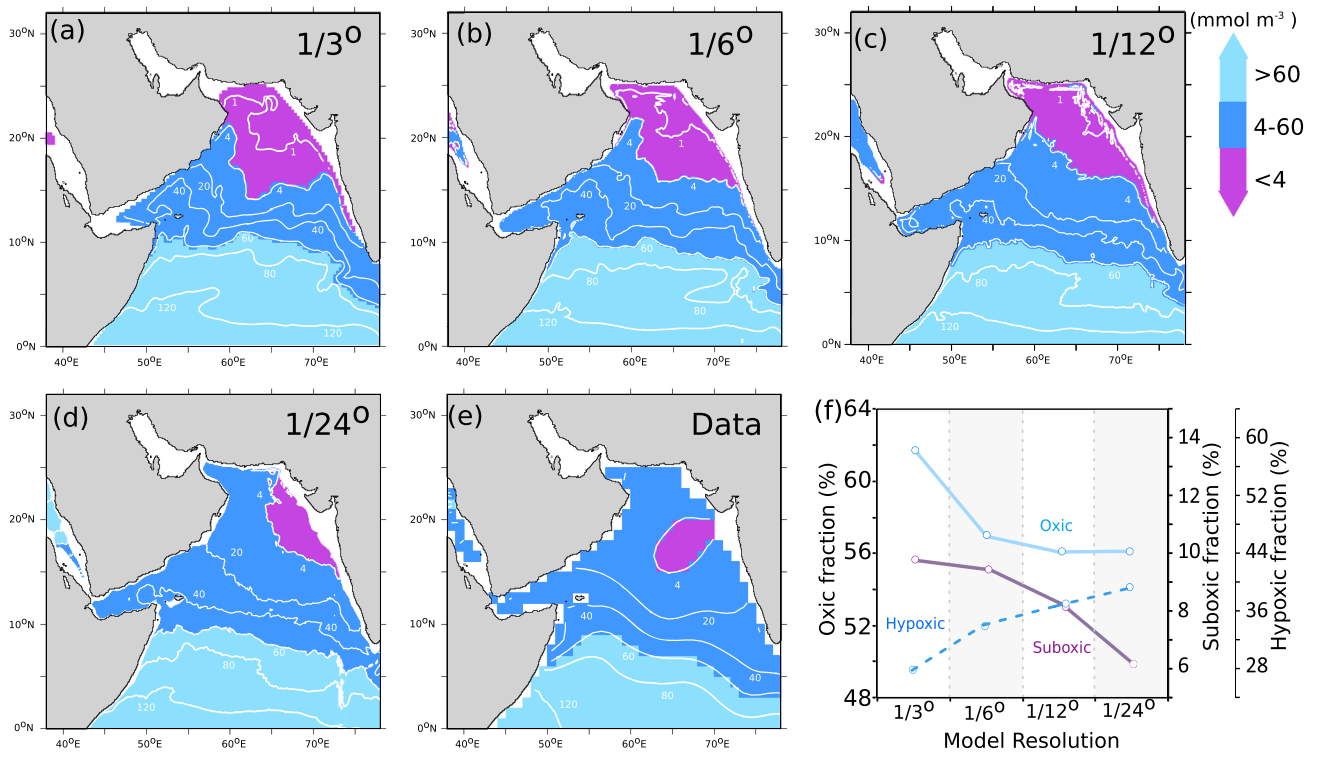

Figure 1. Horizontal distributions and volume fractions of oxic and suboxic conditions in the Arabian Sea. O_2 concentrations at 250 m depth in winter (December–February) in the Arabian Sea as simulated at (a) 1/3°, (b) 1/6°, (c) 1/12°, (d) 1/24°, and (e) from World Ocean Atlas 2009 data set. (f) Oxic, suboxic, and hypoxic ($4 < O_2 < 60$ mmol m^{-3}) volume fractions as simulated at different resolutions in the top 1000 m.

A more detailed evaluation of this simulation shows that the model reproduces relatively well the observed seasonal variability of the surface circulation and in particular the seasonal reversal of the Somali Current (Figure S4 in the supporting information). Furthermore, the magnitude and the spatial distribution of the eddy activity are generally well captured by the model (Figure S5 in the supporting information). The model also successfully captures the observed sea surface height anomalies and sea surface temperature patterns and reproduces generally well the temperature and salinity distributions in the subsurface (see Figures S6–S11 in the supporting information). Similarly, simulated biological variables such as surface chlorophyll *a*, nitrate, and oxygen show a decent agreement with observations in both seasons despite some local biases in the northern Arabian Sea (see Figures S12–S16 in the supporting information). In particular, the location and the intensity of oxygen minimum zone (OMZ) is relatively well reproduced. A more detailed description of the model evaluation is provided in the supporting information.

3. Effects of Eddies on O_2 Distributions and Denitrification

In the coarse resolution simulations, suboxic waters (here, $O_2 < 4$ mmol m^{-3}) fill vast swaths of the northern Arabian Sea at depth, in disagreement with observations that indicate suboxia is limited to a region in the northeastern Arabian Sea (Figure 1). On the other hand, the coarse resolution simulations also overestimate the spatial extent of oxic waters (here $O_2 > 60$ mmol m^{-3}) in the southern Arabian Sea in comparison with observations (Figure 1). With horizontal resolution refinement, the oxygen distribution at depth gradually improves: the extent of suboxia contracts and that of hypoxia ($O_2 < 60$ mmol m^{-3}) expands, resulting in the observed compression of habitats of oxygen-sensitive species. These changes that improve model agreement with observations are also associated with a dampening of horizontal oxygen gradients (Figure 1; see also Figure S17 in the supporting information). Relative to the coarse (1/3°) resolution simulation, the volume of suboxic waters in the highest-resolution (1/24°) simulation is reduced by 38% in the top 1000 m. Additionally, the volume of oxic waters, and hence the potential habitat size, is reduced by around 10% in the same layer (Figure 1e).

In order to identify what drives these changes, we performed a budget analysis of oxygen over the full duration (20 years) of each of the four simulations. We analyzed the oxygen accumulation (time integral) and sources and sinks in each experiment in common volumes defined by the location of suboxic and oxic conditions in the 1/3° simulation, considered here as the reference run. In the suboxic region, the physical and biological sources and sinks of oxygen are generally much larger in magnitude than the oxygen accumulation rates, reflecting a partial compensation of the effects of biology and transport there. Under suboxic conditions, increased resolution leads to both increased biological consumption of oxygen and increased replenishment through lateral transport (Figure 2a), with the latter winning out over the former, resulting in a net accumulation of oxygen in the northern and northeastern Arabian Sea that is proportional to the resolution refinement. In contrast to changes in suboxia that arise from the opposing effects of enhanced ventilation and increased biological consumption, the compression of the volume of oxic waters is essentially driven by enhanced biological consumption of oxygen (Figure 2b). The total transport (i.e., advection and mixing) of oxygen in oxic regions remains nearly independent of resolution, as changes in the horizontal and vertical components of the transport compensate one another (see Table S2 in the supporting information).

The accumulation of dissolved O_2 in the northern Arabian Sea leads to a compression of the volume of suboxia and a reduction of denitrification as more eddy activity is resolved. Indeed, the annually integrated denitrification rate drops from 1.43 T mol N yr^{-1} in the lowest resolution model to 0.95 T mol N yr^{-1} in the highest-resolution version (Figure 2c), a reduction of 35%.

4. Biogeochemical and Ecological Feedbacks of Reduced Denitrification

The eddy-induced reduction in denitrification increases the nitrate supply in the subsurface, contributing to an increase in primary production by 35% in the northeastern Arabian Sea and by 14% in the rest of the domain in the highest resolution simulation, relative to the 1/3° reference case (Figures 2c and S18 in the supporting information). In order to quantify the feedbacks of reduced denitrification on biological productivity and oxygen, we performed four additional simulations at the same resolutions but with denitrification turned off. Without denitrification, primary production increases by only 8% in the northern Arabian Sea and by 10% in the rest of the domain as the resolution is increased from 1/3° to 1/24° (Figure 2c), driven mostly by an increase in vertical supply of nitrate to the euphotic zone, consistent with previous studies [*Resplandy et al.*, 2012]. However, the concomitant increase in remineralization occurs high in the water column, leaving oxygen consumption in the suboxic region nearly unchanged with increasing resolution (see Figure S19 in the supporting information). The unopposed increase in lateral eddy transport therefore results in a substantially larger oxygen accumulation in the higher-resolution simulation (Figure 3a).

On the other hand, when denitrification is allowed, the reduction in the suboxic volume favors aerobic remineralization and hence the consumption of oxygen, which attenuates the effect of eddy-driven ventilation in the suboxic region of the reference run (Figure 2a and S20 in the supporting information). As in the suboxic region, most of the change in oxygen biological consumption in the oxic layer is a consequence of reduced denitrification (Figure 3b). Thus, the eddy-driven ventilation of suboxic waters in the northern Arabian Sea also affects the extent of hypoxic and oxic regions via denitrification suppression.

In an attempt to test the robustness of our results with respect to the assumptions associated with the employed biogeochemical model, and its parameterization of denitrification, we performed three additional experiments where we varied the resolution from 1/3° to 1/12° using the BioEBUS model *Gutknecht et al.* [2013]. This is a higher-complexity biogeochemical model that has two phytoplankton groups and two zooplankton groups as well as a more complex representation of key nitrogen transformations, such as nitrification, denitrification and anamox. The results from these three simulations are consistent with our findings based on the NPZD model. Indeed, we find that the suboxic volume decreases by 22% when the resolution is increased from 1/3° to 1/12°. As a consequence, nitrogen losses due to denitrification and anamox are substantially reduced between the two runs by more than 25%. Finally, we also find a compression of the volume of oxic waters of 8.5%, consistent with our findings using the simpler NPZD model (see Table S3 in the supporting information).

5. Mechanisms of OMZ Ventilation by Eddies

To elucidate the mechanisms of enhanced eddy-induced ventilation, we consider the sensitivity of the meridional volume transport to model resolution. The analysis of transport in depth and density coordinates shows,

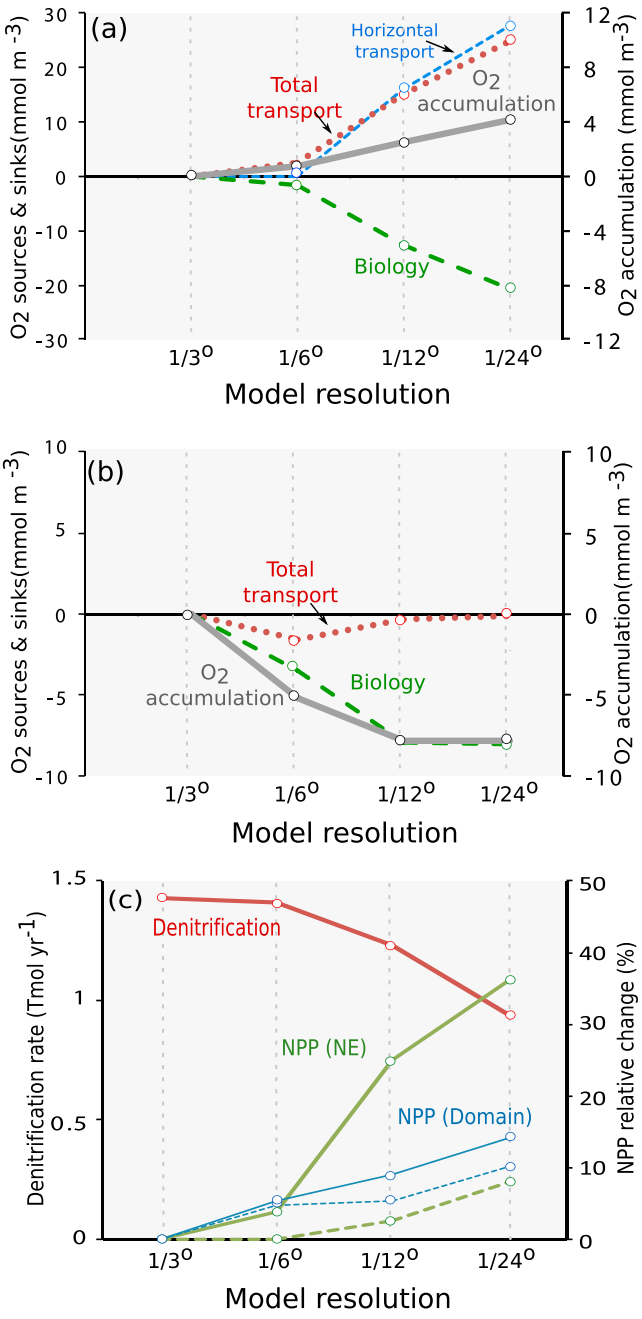

Figure 2. Oxygen budgets in suboxic and oxic layers and denitrification in the Arabian Sea. Changes in time-integrated O_2 accumulation (right axis) and cumulative sources and sinks (left axis) at different resolutions with respect to the (1/3°) coarse resolution model in the (a) suboxic and (b) oxic layers (computed in the 1/3° simulation). (c) Denitrification rate (red) and the increase in net primary production in the northeastern (NE) Arabian Sea (green) and in the rest of the domain (blue) with respect to the coarse resolution simulation with (solid) and without (dashed) active denitrification at different resolutions. Total transport is defined as the sum of the vertical and horizontal advective and mixing fluxes. The northeastern (NE) Arabian Sea is defined as the region east of 60°E and north of 16°N.

however, a weak meridional circulation in the Arabian Sea (north of 8°N) and very limited changes between the high- and low-resolution simulations (see Figures S21 and S22 in the supporting information). This analysis suggests a limited effect of eddies on the mean meridional circulation in the Arabian Sea and fails to capture the role of eddies in O_2 transport. To overcome this difficulty, we propose a novel approach where the meridional transport is binned by O_2 classes for each model resolution.

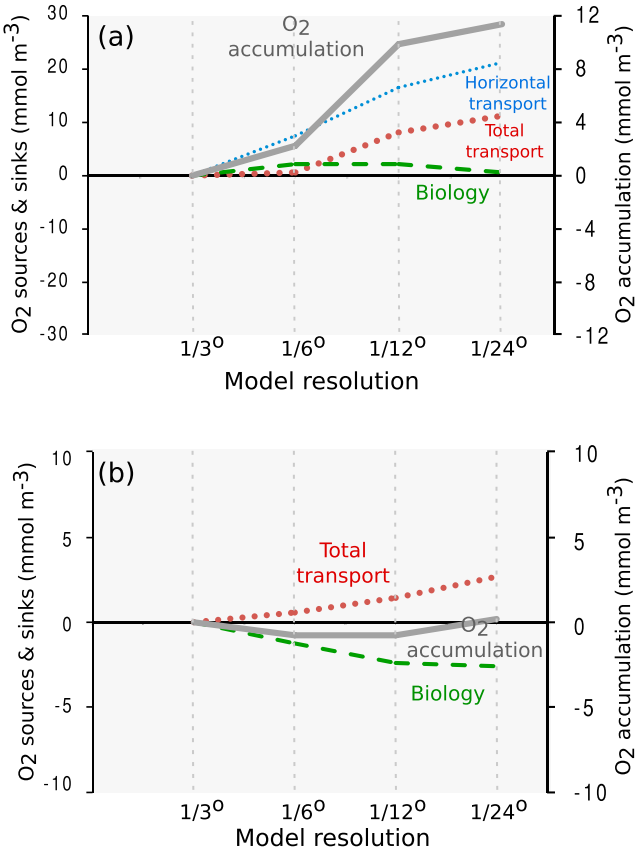

Figure 3. Oxygen budgets in suboxic and oxic layers in the no-denitrification runs. Changes in O_2 sources and sinks (left axis) and accumulation (right axis) with respect to the (1/3°) coarse resolution model in the (a) suboxic and (b) oxic layers simulated at different resolutions in the absence of denitrification.

5.1. Transport in Oxygen Classes: Method

We define the meridional stream function in oxygen "coordinates" as

$$\Psi(y,\hat{O}_2) = \frac{1}{T}\iiint v\mathcal{H}(\hat{O}_2 - O_2(x,y,z,t))\,dx\,dz\,dt \tag{1}$$

where v is the meridional velocity, $O_2(x,y,z,t)$ is the oxygen concentration at a given location and time, T is the period over which the circulation is averaged, and $\mathcal{H}(\hat{O}_2 - O_2(x,y,z,t))$ is the Heaviside function defined as

$$\mathcal{H}(\hat{O}_2 - O_2(x,y,z,t)) = \begin{cases} 1, & \text{if } O_2(x,y,z,t) \le \hat{O}_2 \\ 0, & \text{otherwise} \end{cases}$$

The oxygen threshold $\hat{O}_2$ is treated as a constant in the integral on right-hand side of (1), and the stream function $\Psi(y,\hat{O}_2)$ is equal to the net meridional volume flux of all water with an oxygen concentration less or equal to $\hat{O}_2$. One can also define the meridional volume transport on a surface of constant oxygen concentration as

$$F(y,\hat{O}_2) = \frac{\partial\Psi}{\partial\hat{O}_2} = \frac{1}{T}\iiint v\delta(\hat{O}_2 - O_2(x,y,z,t))\,dx\,dz\,dt, \tag{2}$$

where $\delta(\hat{O}_2 - O_2(x,y,z,t))$ is the Dirac-delta function defined as

$$\delta(\hat{O}_2 - O_2(x,y,z,t)) = \frac{\partial\mathcal{H}(\hat{O}_2 - O_2(x,y,z,t))}{\partial\hat{O}_2}.$$

The formulation of a stream function like (1), or equivalently a tracer-based transport like (2), is more typically defined in terms of a quantity that is related monotonically to depth, such as density, and in this case is equivalent to the thickness-weighted average formulation of *Young* [2012]. However, it is also well defined in terms

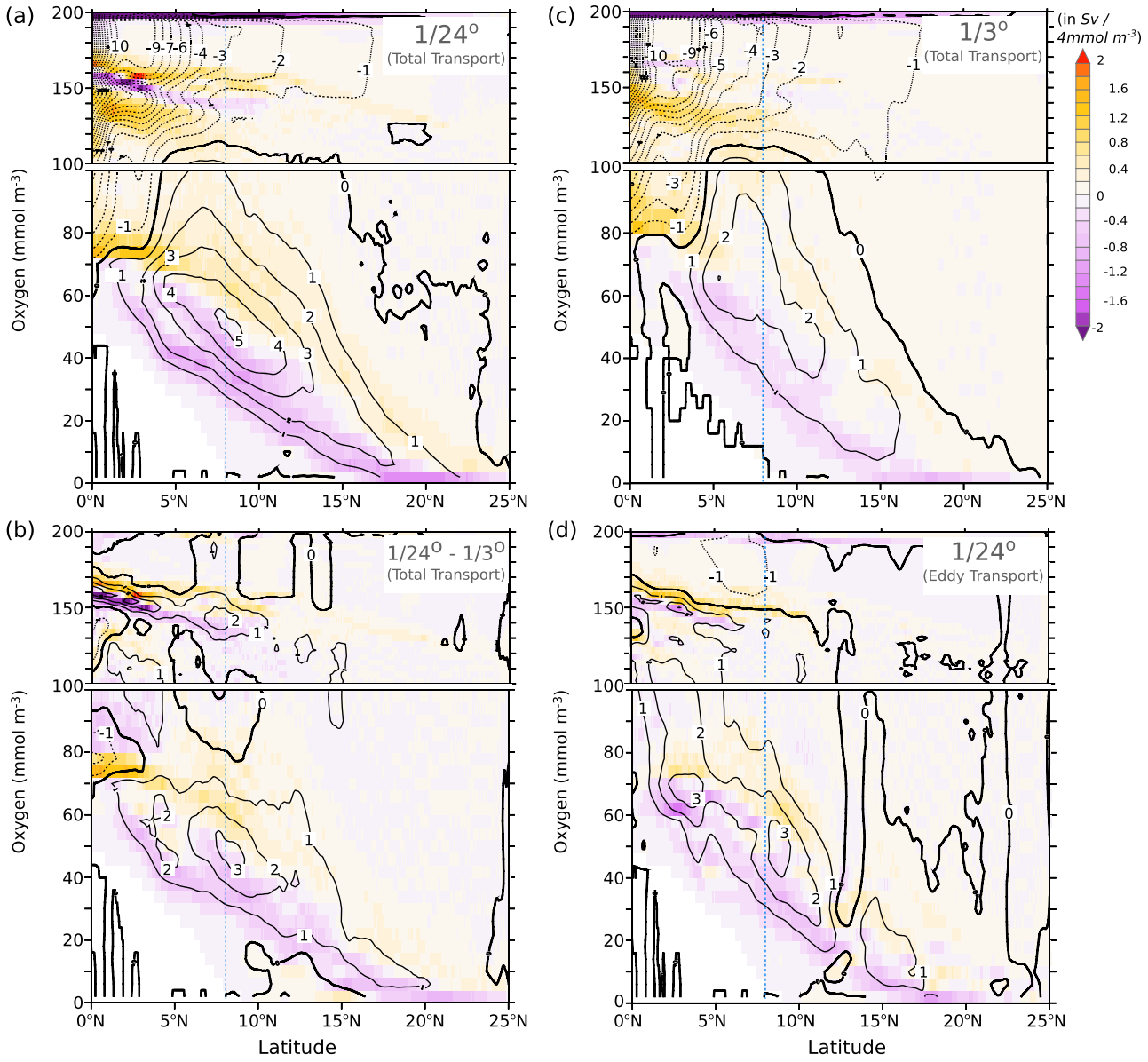

Figure 4. Meridional circulation in the Arabian Sea in O_2 coordinates. Meridional stream function from (1), in Sv, from (a) the 1/24° simulation, (b) the 1/3° simulation, (c) the difference between 1/24° and 1/3° simulations, and (d) the eddy component of the transport in the 1/24° simulation. Contour lines indicate the meridional stream function (positive indicates clockwise circulation). The color shading shows the meridional component of the transport (in Sv; 4 mmol O_2 m^{-3}). The vertical blue dashed line indicates the latitude of the southern tip of India.

of a nonmonotonic coordinate, such as oxygen. Examples in the atmospheric literature include transport in terms of moist potential temperature [*Pauluis et al.*, 2008; *Laliberté et al.*, 2015] and in oceanography in terms of temperature and salinity [*Zika et al.*, 2012]. Intuition for this analysis is developed through its use below and in the supporting information.

The oxygen concentration and the meridional velocity can be decomposed as the sum of their mean and eddy components as

$$O_2(x,y,z,t) = \overline{O_2}(x,y,z,t) + O_2'(x,y,z,t),$$

$$v(x,y,z,t) = \overline{v}(x,y,z,t) + v'(x,y,z,t),$$

where the overline indicates a 3 month running mean. Similarly, by decomposing the stream function into contributions from the mean and eddy field, the eddy stream function can be written as

$$\Psi'(y,\hat{O}_2) = \Psi(y,\hat{O}_2) - \overline{\Psi}(y,\hat{O}_2)$$

with

$$\overline{\Psi}(y,\hat{O}_2) = \frac{1}{T}\iiint \overline{v}\mathcal{H}(\hat{O}_2 - \overline{O_2}(x,y,z,t))\,dx\,dz\,dt$$

5.2. Transport in Oxygen Classes: Results

In practice, to estimate the meridional mass flux $\overline{vh}(y,\hat{O}_2)$, where h is the thickness of the layer with oxygen concentration $\hat{O}_2$, we binned model outputs at high temporal frequency (3 day model outputs over 5 years) onto 62 oxygen bins (using 124 oxygen bins yielded identical results) ranging from 0 to 248 mmol m^{-3} and then summed the transport zonally and in time.

Figure 4 shows that water enters the Arabian Sea at 8°N with O_2 concentration ranging between 80 mmol m^{-3} and 150 mmol m^{-3}. This is balanced by an export of (i) surface water with high-O_2 concentration above 160 mmol m^{-3} and (ii) hypoxic water ($O_2 < 60$ mmol m^{-3}) at depth. The ventilation of the OMZ can be quantified in terms of the volume of hypoxic water exported out of the Arabian Sea. This transport goes from 2 sverdrup (Sv) to 5 Sv when the resolution is increased from 1/3° to 1/24°. By applying a 3 month running average to 3 day model outputs, we also decompose the total transport into one part that is driven by the mean flow and another part that is driven by the time-varying fluctuations in velocity and oxygen (see section2). At relatively low oxygen, the eddy-driven component of the meridional transport is of comparable magnitude to the transport changes that arise from resolution refinement. This suggests that the enhanced ventilation of the OMZ is driven to a large extent by the effect of transient eddies, while changes in the mean circulation between the high- and low-resolution simulations appear to play a relatively minor role (Figure 4). Additionally, the contrast between the large eddy transport estimated in O_2 coordinates and the substantially smaller transport in isopycnal coordinates (see Figure S22 in the supporting information) suggests that most of the eddy transport occurs along isopycnal surfaces.

6. Discussion and Conclusions

Overall, the set of model experiments presented in this study provides strong evidence for the role of eddies in shaping the extent and magnitude of important oxygen classes in the Arabian Sea. This has strong biogeochemical and ecological implications for the region and potentially the globe. First, the reduction in suboxia induced by eddies also suppresses denitrification, thus increasing locally biological production and influencing the nitrogen cycle at regional and global scales. Second, the productivity enhancement associated with these changes leads to an increase in oxygen consumption that compresses the potential habitats of hypoxia-intolerant species. Thus, eddies impact the Arabian Sea ecosystem both at the level of microorganisms (e.g., plankton and denitrifying bacteria) as well as at the level of higher trophic animals (e.g., fish) that are stressed in low-oxygen environments. Eddies might have similar effects in other OMZs, and the contrasts in eddy activity between different regions and over time can contribute to the observed spatial and temporal variability in OMZs.

The demonstrated importance of eddy fluxes in shaping low-oxygen regions provokes the following question: why do global ocean models, with parameterized eddy fluxes, fail to accurately represent OMZs? This is evidenced by a number of studies showing that coarse resolution, noneddy resolving ocean models, typically overpredict the extent and magnitude of OMZs, in particular, in the Pacific Ocean [e.g., *Bopp et al.*, 2013; *Cocco et al.*, 2013; *Cabré et al.*, 2015]. In section 5 we demonstrated that the increase with model resolution of eddy-driven isopycnal transport of oxygen occurs with little change to the mean isopycnal structure, implying that increased eddy activity can affect along-isopycnal transport and isopycnal flattening at different rates. This is consistent with *Gnanadesikan et al.* [2013], who argue that the Redi coefficient (which parameterizes along-isopycnal tracer mixing) should be set to larger values than the Gent-McWilliams coefficient (following *Griffies* [1998], the two coefficients are set equal in almost all climate models). Moreover, *Abernathey et al.* [2013] explicitly diagnose the two coefficients in a high-resolution channel model simulations, finding that the former exceeds the latter by more than a factor of 2.

A major goal of the present work is to focus on the detailed nature of resolved eddy fluxes of oxygen (in a particular region, the Arabian Sea), partially in order to better understand how to improve parameterizations of these fluxes in global earth system models. This will be addressed in coming papers.

Acknowledgments
Support for this research has come from the Center for Prototype Climate Modeling (CPCM), the New York University Abu Dhabi (NYUAD) Research Institute. Computations were performed at the High Performance cluster (HPC) of NYUAD, Butinah. We thank B. Marchand and M. Barwani from the NYUAD HPC team for technical support. We are thankful to N. Gruber for allowing access to the biogeochemical model code. The authors declare that they have no competing financial interests. The data used for forcing and validating the model are publicly available online and can be accessed from cited references. The model code can be accessed online at http://www.romsagrif.org. The model outputs are available from the authors upon request.

References

Abernathey, R., D. Ferreira, and A. Klocker (2013), Diagnostics of isopycnal mixing in a circumpolar channel, *Ocean Model.*, *72*, 1–16.
Barnier, B., L. Siefridt, and P. Marchesiello (1995), Thermal forcing for a global ocean circulation model using a three-year climatology of ECMWF analyses, *J. Mar. Syst.*, *6*(4), 363–380.
Bettencourt, J. H., C. López, E. Hernández-García, I. Montes, J. Sudre, B. Dewitte, A. Paulmier, and V. Garçon (2015), Boundaries of the Peruvian oxygen minimum zone shaped by coherent mesoscale dynamics, *Nat. Geo.*, *8*, 937–940.
Brandt, P., et al. (2015), On the role of circulation and mixing in the ventilation of oxygen minimum zones with a focus on the eastern tropical North Atlantic, *Biogeosciences*, *12*, 489–512, doi:10.5194/bg-12-489-2015.
Bopp, L., et al. (2013), Multiple stressors of ocean ecosystems in the 21st century: Projections with CMIP5 models, *Biogeosciences*, *10*, 6225–6245, doi:10.5194/bg-10-6225-2013.
Cabré, A., I. Marinov, R. Bernardello, and D. Bianchi (2015), Oxygen minimum zones in the tropical Pacific across CMIP5 models: Mean state differences and climate change trends, *Biogeosciences*, *12*(18), 5429–5454.
Cocco, V., et al. (2013), Oxygen and indicators of stress for marine life in multi-model global warming projections, *Biogeosciences*, *10*, 1849–1868, doi:10.5194/bg-10-1849-2013.
Codispoti, L., J. A. Brandes, J. Christensen, A. Devol, S. Naqvi, H. W. Paerl, and T. Yoshinari (2001), The oceanic fixed nitrogen and nitrous oxide budgets: Moving targets as we enter the anthropocene?, *Sci. Mar.*, *65*(S2), 85–105.
da Silva, A. M., C. C. Young, and S. Levitus (1994), Atlas of surface marine data 1994, vol. 4: Anomalies of fresh water fluxes.
Duteil, O., F. U. Schwarzkopf, C. W. Böning, and A. Oschlies (2014), Major role of the equatorial current system in setting oxygen levels in the eastern tropical Atlantic Ocean: A high-resolution model study, *Geophys. Res. Lett.*, *41*, 2033–2040, doi:10.1002/2013GL058888.
Falkowski, P. G., D. Ziemann, Z. Kolber, and P. K. Bienfang (1991), Role of eddy pumping in enhancing primary production in the ocean, *Nature*, *352*, 55–58, doi:10.1038/352055a0.
Gent, P. R., and J. C. McWilliams (1990), Isopycnal mixing in ocean circulation models, *J. Phys. Oceanogr.*, *20*, 150–155.
Gnanadesikan, A., D. Bianchi, and M.-A. Pradal (2013), Critical role for mesoscale eddy diffusion in supplying oxygen to hypoxic ocean waters, *Geophys. Res. Lett.*, *40*(19), 5194–5198.
Gray, J. S., R. S.-s. Wu, and Y. Y. Or (2002), Effects of hypoxia and organic enrichment on the coastal marine environment, *Mar. Ecol. Prog. Ser.*, *238*(1), 249–279.
Griffies, S. M. (1998), The Gent-McWilliams skew flux, *J. Phys. Oceanogr.*, *28*, 831–841.
Gruber, N. (2011), Warming up, turning sour, losing breath: Ocean biogeochemistry under global change, *Philos. Trans. R. Soc. A*, *369*(1943), 1980–1996.
Gruber, N., H. Frenzel, S. C. Doney, P. Marchesiello, J. C. McWilliams, J. R. Moisan, J. J. Oram, G.-K. Plattner, and K. D. Stolzenbach (2006), Eddy-resolving simulation of plankton ecosystem dynamics in the California Current System, *Deep Sea Res. I*, *53*(9), 1483–1516.
Gruber, N., Z. Lachkar, H. Frenzel, P. Marchesiello, M. Münnich, J. C. McWilliams, T. Nagai, and G.-K. Plattner (2011), Eddy-induced reduction of biological production in eastern boundary upwelling systems, *Nat. Geo.*, *4*(11), 787–792.
Gutknecht, E., et al. (2013), Coupled physical/biogeochemical modeling including O_2-dependent processes in the eastern boundary upwelling systems: Application in the Benguela, *Biogeosciences*, *10*(6), 3559–3591.
Lachkar, Z., and N. Gruber (2011), What controls biological production in coastal upwelling systems? Insights from a comparative modeling study, *Biogeosciences*, *8*(10), 2961–2976.
Laliberté, F., J. Zika, L. Mudryk, P. J. Kushner, J. Kjellsson, and K. Döös (2015), Constrained work output of the moist atmospheric heat engine in a warming climate, *Science*, *347*(6221), 540–543.
Large, W. G., J. C. McWilliams, and S. C. Doney (1994), Oceanic vertical mixing: A review and a model with a nonlocal boundary layer parameterization, *Rev. Geophys.*, *32*(4), 363–403.
Lathuilière, C., V. Echevin, M. Lévy, and G. Madec (2010), On the role of mesoscale circulation on an idealized coastal upwelling ecosystem, *J. Geophys. Res.*, *115*, C09018, doi:10.1029/2009JC005827.
Lathuilière, C., M. Lévy, and V. Echevin (2011), Impact of eddy-driven vertical fluxes on phytoplankton abundance in the euphotic layer, *J. Plankton Res.*, *33*(5), 827–831.
Lévy, M., P. Klein, and A.-M. Treguier (2001), Impact of sub-mesoscale physics on production and subduction of phytoplankton in an oligotrophic regime, *J. Mar. Res.*, *59*(4), 535–565.
Marchesiello, P., L. Debreu, and X. Couvelard (2009), Spurious diapycnal mixing in terrain-following coordinate models: The problem and a solution, *Ocean Model.*, *26*(3), 156–169.
McCreary, J. P., Z. Yu, R. R. Hood, P. Vinaychandran, R. Furue, A. Ishida, and K. J. Richards (2013), Dynamics of the Indian-Ocean oxygen minimum zones, *Prog. Oceanogr.*, *112*, 15–37.
McGillicuddy, D., A. Robinson, D. Siegel, H. Jannasch, R. Johnson, T. Dickey, J. McNeil, A. Michaels, and A. Knap (1998), Influence of mesoscale eddies on new production in the Sargasso Sea, *Nature*, *394*(6690), 263–266.
Oschlies, A., and V. Garçon (1998), Eddy-induced enhancement of primary production in a model of the North Atlantic Ocean, *Nature*, *394*(6690), 266–269.
Pauluis, O., A. Czaja, and R. Korty (2008), The global atmospheric circulation on moist isentropes, *Science*, *321*, 1075–1078.
Resplandy, L., M. Lévy, G. Madec, S. Pous, O. Aumont, and D. Kumar (2011), Contribution of mesoscale processes to nutrient budgets in the Arabian Sea, *J. Geo. Res. Oce.*, *116*, C11007, doi:10.1029/2011JC007006.
Resplandy, L., M. Lévy, L. Bopp, V. Echevin, S. Pous, V. Sarma, and D. Kumar (2012), Controlling factors of the oxygen balance in the Arabian Sea's OMZ, *Biogeosciences*, *9*(12), 5095–5109.
Risien, C. M., and D. B. Chelton (2008), A global climatology of surface wind and wind stress fields from eight years of QuikSCAT scatterometer data, *J. Phys. Oceanogr.*, *38*(11), 2379–2413.
Shchepetkin, A. F., and J. C. McWilliams (2005), The Regional Oceanic Modeling System (ROMS): A split-explicit, free-surface, topography-following-coordinate oceanic model, *Ocean Model.*, *9*(4), 347–404.
Smith, W. H., and D. T. Sandwell (1997), Global sea floor topography from satellite altimetry and ship depth soundings, *Science*, *277*(5334), 1956–1962.
Vaquer-Sunyer, R., and C. M. Duarte (2008), Thresholds of hypoxia for marine biodiversity, *Proc. Natl. Acad. Sci.*, *105*(40), 15,452–15,457.
Young, W. R. (2012), An exact thickness-weighted average formulation of the Boussinesq equations, *J. Phys. Oceanogr.*, *42*, 692–707.
Zika, J. D., M. H. England, and W. P. Sijp (2012), The ocean circulation in thermohaline coordinates, *J. Phys. Oceanogr.*, *42*, 708–724.